Magnetic Properties of $[(H_2O)_2M\{(OH)_2Coen_2\}_2](X)_2\cdot nH_2O$ (M=Ni or Co, X=SO_4 or S_2O_6 and n=5 or 7)

Hanako KOBAYASHI, Kazuo OHKI, Ikuji TSUJIKAWA, Keiji OSAKI,* and Norikiyo URYÛ*

Faculty of Science, Kyoto University, Sakyo-ku, Kyoto 606

**Faculty of Engineering, Kyushu University, Hakozaki, Fukuoka 812*

(Received October 8, 1975)

The magnetic properties of $[(H_2O)_2Ni\{(OH)_2Coen_2\}_2](SO_4)_2\cdot 7H_2O$, $[(H_2O)_2Co\{(OH)_2Coen_2\}_2](SO_4)_2\cdot 5H_2O$, $[(H_2O)_2Co\{(OH)_2Coen_2\}_2](SO_4)_2\cdot 7H_2O$, and $[(H_2O)_2Co\{(OH)_2Coen_2\}_2](S_2O_6)_2\cdot 5H_2O$ were investigated on powder samples. The paramagnetism of these compounds was considered to be that of the central Ni^{2+} or Co^{2+} ion. From the fits of the experimental data with the calculated magnetic susceptibilities and the simulations of the ESR derivative curves, the ligand field parameters and g-values were determined. The ligand field around the Co^{2+} ion in $[(H_2O)_2Co\{(OH)_2Coen_2\}_2](SO_4)_2\cdot 5H_2O$ was concluded to be tetragonal and in the other samples the ligand fields at the central divalent ions were found to be rhombic.

Werner[1] obtained a series of tri-nuclear $[(H_2O)_2Co\{(OH)_2Coen_2\}_2]$ salts from the partly oxidized mixtures of cobalt(II) salts and ethylendiamine. Cambi[2] later observed the magnetic susceptibility of the sulfate at room temperature. The main structure of the complex ion is considered to be a Co^{2+} ion linked to two Co^{3+} ions on wings through double OH bridges. Two other ligand sites for the central Co^{2+} ion are occupied by two H_2O molecules and four other ligand sites of each Co^{3+} ion by two ethylendiamines, as shown in Fig. 1. The magnetic properties of such complex compounds with mixed valencies are of interest because the magnetic properties of the mixed valency compounds[3,4] are not well known, except for the double exchange interaction in mixed compounds of $LaMnO_3$ and $BaMnO_3$.[3] In the course of this investigation, a new method of synthesis of this kind of complex compound was discovered by Mori *et al.*[5] in which $[(H_2O)_2M\{(OH)_2Coen_2\}_2]X_2\cdot nH_2O$, where $M=Ni^{2+}$, Co^{2+}, Mg^{2+}, Zn^{2+} or Cd^{2+}, $X=SO_4^{2-}$, $S_2O_3^{2-}$ or $S_2O_6^{2-}$ and n=5 or 7, were synthesized. Samples synthesized by the new method were offered by Mori *et al.* for the present investigation.

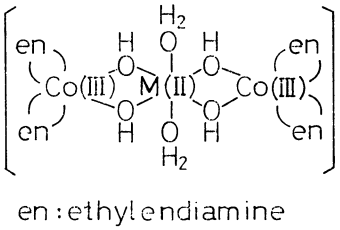

Fig. 1. The schema of $[(H_2O)_2M\{(OH)_2Coen_2\}_2]^{4+}$ complex ion.

In the present paper, the magnetic properties of $[(H_2O)_2Ni\{(OH)_2Coen_2\}_2](SO_4)_2\cdot 7H_2O$, $[(H_2O)_2Co\{(OH)_2Coen_2\}_2](SO_4)_2\cdot 5H_2O$, $[(H_2O)_2Co\{(OH)_2Coen_2\}_2](SO_4)_2\cdot 7H_2O$ and $[(H_2O)_2Co\{(OH)_2Coen_2\}_2](S_2O_6)_2\cdot 5H_2O$ are examined. Mori *et al.*[5] observed the reflection spectra of these salts on powder. The d-d bands of the magnetic central Ni^{2+} or Co^{2+} ions were not discernible because of the much smaller absorptivity in comparison with those of the d-d bands of the trivalent cobalt chromophores. It was, therefore, impossible to determine the orbital energy levels by optical measurements.

Experimental

Preparation of Samples. $[(H_2O)_2M(II)\{(OH)_2Coen_2\}_2](SO_4)_2\cdot nH_2O$ with M=Mg, Co, Ni(n=7) and Zn, Cd (n=5) were prepared according to the method of Mori *et al.*[5] The new procedure gave only this product with seven molecules of water of crystallization for the salt of M=Co, so that $[(H_2O)_2Co\{(OH)_2Coen_2\}_2](SO_4)_2\cdot 5H_2O$ was prepared according to the original method of Werner *et al.* with a slight modification. One hundred and forty-five grams of cobalt(II)sulfate heptahydrate were dissolved in 180 ml of water, and 300 ml of a 10% ethylenediamine aqueous solution was added to it. After about four hours, a green precipitate, with a pink precipitate, was filtered off. From the filtrate a massive amount of pink silky crystals soon began to precipitate. The silky precipitate was filtered through a glass filter and washed with water. Then the precipitate was placed between unglazed plates (Ton platten).

The results of the chemical analysis are as follows. For $[(H_2O)_2M(II)\{(OH)_2Coen_2\}_2](SO_4)_2\cdot 7H_2O$, Found: M=Mg(II), 3.07; Co(III), 14.13%. Calcd for: Mg(II), 3.02; Co(III), 14.13%. Found: M=Co(II), 7.01; Co(III), 13.65%. Calcd for: Co(II), 7.02; Co(III), 14.04%. Found: M=Ni(II), 6.69; Co(III), 13.38%. Calcd for: Ni(II), 7.00; Co(III), 13.38%. Found: M=Zn(II), 7.79; Co(III), 13.49%. Calcd for: Zn(II), 8.07; Co(III), 14.55%. Found: M=Cd(II), 13.25; Co(III), 13.82%. Calcd for: Cd(II), 13.12; Co(III), 13.75%. For $[(H_2O)_2Co\{(OH)_2Coen_2\}_2](SO_4)_2\cdot 5H_2O$, Found: H, 6.21; C, 11.17; Co, 21.33; N, 13.37%. Calcd for: H, 6.28; C, 11.98; Co, 22.02; N, 13.95%, and for $[(H_2O)_2Co\{(OH)_2Coen_2\}_2](S_2O_6)_2\cdot 5H_2O$, Found: H, 4.96; Co, 23.06; N, 12.31%. Calcd for: H, 5.41; Co, 22.96; N, 12.03%.

The hepta hydrate of $[(H_2O)_2Co\{(OH)_2Coen_2\}_2](SO_4)_2$ prepared from the penta hydrate by the Werner method did not give good analytical values.

Magnetic Susceptibilities. Magnetic susceptibilities at liquid helium and liquid hydrogen temperatures were measured with a Hartshorn alternating current bridge. A Faraday magnetic balance with a field strength of *ca.* 9000 Oe was also employed for magnetic susceptibilities between 4.2 K and room temperature. The magnetic susceptibility of anhydrous hexaamminechromium(III) chloride powder was used as a "thermometer" which was calibrated at each run to an atmospheric liquid helium temperature with corrections for the Hg-barometer and gravitational constant following procedure of Linder.[6] The accuracy for all the measure-

Table 1. Diamagnetic part of the magnetic susceptibility per mole (cgs emu)

Compound	Estimated from expt	Calcd by Pascal's rule
$[(H_2O)_2Zn\{(OH)_2Coen_2\}_2](SO_4)_2\cdot 5H_2O$	−0.00041	−0.00036
$[(H_2O)_2Co\{(OH)_2Coen_2\}_2](SO_4)_2\cdot 5H_2O$	−0.00042	−0.00037
$[(H_2O)_2Mg\{(OH)_2Coen_2\}_2](SO_4)_2\cdot 7H_2O$	−0.00031	−0.00038
$[(H_2O)_2Ni\{(OH)_2Coen_2\}_2](SO_4)_2\cdot 7H_2O$	−0.00032	−0.00040
$[(H_2O)_2Co\{(OH)_2Coen_2\}_2](SO_4)_2\cdot 7H_2O$	−0.00033	−0.00040

ments was not less than 5% in the case of the AC bridge method and 10% in the case of the Faraday method.

Taking into account the isomorphism[5] of the sulfates with the same number of water molecules of crystallization, the corrections for the diamagnetic part of the susceptibilities were performed as follows: for the estimation of the diamagnetic part of the susceptibility of $[(H_2O)_2Co\{(OH)_2Coen_2\}_2](SO_4)_2\cdot 5H_2O$, e.g., the diamagnetic susceptibility of a free Zn^{2+} ion in the literature[7] was subtracted from the observed susceptibility at room temperature for $[(H_2O)_2Zn\{(OH)_2Coen_2\}_2](SO_4)_2\cdot 5H_2O$, then the diamagnetic susceptibility of a free Co^{2+} ion was added. A similar correction for the heptahydrate salts was made using the observed susceptibility of $[(H_2O)_2Mg\{(OH)_2Coen_2\}_2](SO_4)_2\cdot 7H_2O$. Table 1 shows these corrections together with the diamagnetic susceptibilities calculated from Pascal's rule.

Electron Spin Resonance. The electron spin resonance of a powder sample was measured using a Japan Electron Optics Laboratory Co., Ltd., JES-3 ESR spectrometer at liquid helium temperatures. X-Band spectra were observed with an 80 Hz modulation of 15 V. The external magnetic field was swept to about 23 kOe. Sixty minutes/3000 Oe scans were usually made.

Results and Discussion

Molar magnetic susceptibilities of $[(H_2O)_2Ni\{(OH)_2Coen_2\}_2](SO_4)_2\cdot 7H_2O$ are shown as a function of temperature in Fig. 2 and Table 2. The compound was paramagnetic down to 1.3 K, *i.e.*, magnetic interactions between magnetic ions in this complex compound are negligibly small compared to the thermal energy except at very low temperatures. The effective Bohr magneton number of 3.17 in the higher temperature region shown in Fig. 3 indicates that the paramagnetism is due to a Ni^{2+} ion, and that the two Co^{3+} ions may be in low spin states of the complex ion. The Ni^{2+} ion is surrounded by six oxygen atoms, of which four oxygen atoms are part of –OH– bridges and two oxygen atoms are part of co-ordinated water molecules, provided we accept the idea of Werner. No preliminary calculations of the temperature dependence of the susceptibility, ignoring the rhombic terms, show any agreement with the observed susceptibility, and therefore, a rhombic symmetry of the ligand field formed by six co-ordinated oxygen atoms was assumed for the components of the magnetic susceptibility. A temperature-independent paramagnetic susceptibility, that is, a high-frequency term, was graphically obtained from extrapolation of the plots of the observed molar mag-

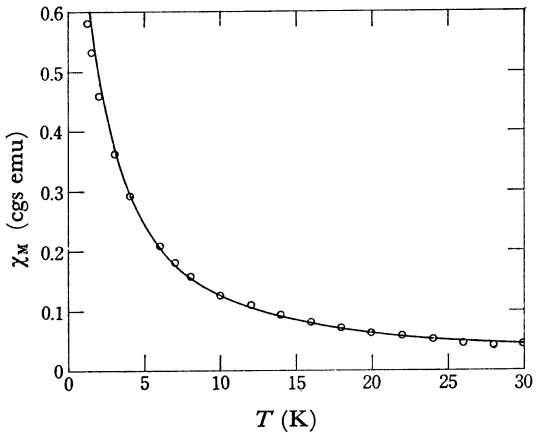

Fig. 2. The molar magnetic susceptibilities of $[(H_2O)_2Ni\{(OH)_2Coen_2\}_2](SO_4)_2\cdot 7H_2O$ (cgs emu) as a function of temperatures (K). ○: Experimental values corrected for the diamagnetic susceptibility and the temperature independent paramagnetic susceptibility. —: Calculated values with parameters, $D=-3.0$ cm^{-1}, $E=-1.0$ cm^{-1}, $g=2.25$ and $\theta=0$.

Table 2. Molar magnetic susceptibilities of $[(H_2O)_2Ni\{(OH)_2Coen_2\}_2](SO_4)_2\cdot 7H_2O$ (cgs emu)

Temp K	χ_M expt	χ_M calcd	Temp K	χ_M expt	χ_M calcd
1.20		(0.5800)	30.0	0.0391	(0.0418)
1.25	0.5799		70.0	0.01885	(0.0179)
2.00	0.4589	(0.4696)	77.0	0.01672	(0.0163)
4.00	0.2909	(0.2850)	100.0	0.01262	(0.0125)
6.00	0.2084	(0.1990)	140.0	0.00922	(0.00898)
10.0	0.1294	(0.1237)	180.0	0.00732	(0.00699)
14.0	0.0949	(0.0888)	220.0	0.00579	(0.005719)
16.0	0.0819	(0.0779)	260.0	0.00456	(0.004839)
18.0	0.0719	(0.0695)	290.0	0.00430	(0.004339)
20.0	0.0629	(0.0626)	293.7	0.00429	

The experimental χ_M values are corrected for the diamagnetic susceptibility and the temperature-independent paramagnetic susceptibility.

The χ_M values calculated from Eq. 2, with $D=-3.0$ cm^{-1}, $E=-1.0$ cm^{-1}, $g=2.25$, and $\theta=-0.1$ K, are shown in parentheses.

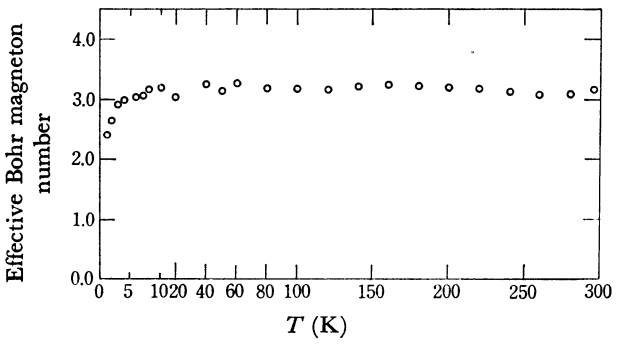

Fig. 3. The effective Bohr magneton numbers of $[(H_2O)_2Ni\{(OH)_2Coen_2\}_2](SO_4)_2\cdot 7H_2O$ *versus* temperatures.

netic susceptibilities *versus* reciprocal temperatures for $1/T \to 0$. The temperature-independent paramagnetic susceptibility per mole was 0.0001 cgs emu., from which the energy difference between the ground orbital state and the first-excited orbital state was estimated to be about 10^4 cm^{-1}.[8] A nickel ion in the nickel Tutton salts is also co-ordinated by six oxygen atoms. In this case, the F state of the nickel ion is split into two triplet and one singlet substates by the cubic ligand field, and the energy splitting between the lowest singlet and the lower triplet is estimated to be about 8000 cm^{-1}. Though it is not known how the lower triplet is further split by the non-cubic ligand field, the temperature-independent paramagnetic susceptibility mentioned above is considered to show a cubic-field splitting similar to that of the nickel Tutton salt. The magnetic susceptibility was calculated, therefore, following the spin Hamiltonian

$$H = DS_z^2 + E(S_x^2 - S_y^2) + g\beta HS, \qquad (1)$$

where D and E are axial and rhombic ligand field parameters, respectively, β is the Bohr magneton and H the applied magnetic field. In order to obtain a molar magnetic susceptibility corrected for the diamagnetic susceptibility and the temperature-independent paramagnetic susceptibility, a fit with a calculated magnetic susceptibility was made assuming fairly small magnetic interactions. The formula[9] used for the calculation, in which the magnetic interaction is considered to be corrected for temperature, is:

$$\chi_{\text{powder}} = \frac{1}{3}(\chi_x + \chi_y + \chi_z), \qquad (2)$$

where

$$\chi_x = \frac{2Ng^2\beta^2}{\frac{D+E}{2}} \frac{\sinh \frac{D+E}{2k(T-\theta)}}{\exp\left(\frac{-3E-D}{2k(T-\theta)}\right) + 2\cosh \frac{D+E}{2k(T-\theta)}},$$

$$\chi_y = \frac{2Ng^2\beta^2}{\frac{D-E}{2}} \frac{\sinh \frac{D-E}{2k(T-\theta)}}{\exp\left(\frac{-3E-D}{2k(T-\theta)}\right) + 2\cosh \frac{D-E}{2k(T-\theta)}},$$

and

$$\chi_z = \frac{2Ng^2\beta^2}{E} \frac{\sinh \frac{E}{k(T-\theta)}}{\exp\left(\frac{D}{k(T-\theta)}\right) + 2\cosh \frac{E}{k(T-\theta)}}.$$

Assuming isotropic g values, a fairly good fit was obtained for $D = -2.9 \sim -3.0$ cm^{-1}, $E = -1.0$ cm^{-1}, $g = 2.25$ and $\theta = -0.1$ K, as is seen in Fig. 2 and Table 2. In conformity with the above values of D and E, the X-band ESR of this sample at 4.2 K gave no signal up to 23 kOe of the applied magnetic field.

The effective Bohr magneton number was 3.17 in the temperature region above 8 K and at lower temperatures it decreased showing the effect of the rhombic ligand field and antiferromagnetic interactions among magnetic complex ions.

The molar magnetic susceptibilities of $[(H_2O)_2Co\{(OH)_2Coen_2\}_2](SO_4)_2 \cdot 5H_2O$, corrected for diamagnetic susceptibility, are shown in Figs. 4a and 4b and Table 3. The compound is paramagnetic down to 1.3 K, *i.e.*, the magnetic interactions among the magnetic ions are very weak, but the temperature dependence of the susceptibility is not simply that of the Curie-

TABLE 3. MOLAR MAGNETIC SUSCEPTIBILITIES (cgs emu)

Temp K	$[(H_2O)_2Co\{(OH)_2Coen_2\}_2](SO_4)_2 \cdot 5H_2O$ χ_M		$[(H_2O)_2Co\{(OH)_2Coen_2\}_2](SO_4)_2 \cdot 7H_2O$ χ_M		$[(H_2O)_2Co\{(OH)_2Coen_2\}_2](S_2O_6)_2 \cdot 5H_2O$ χ_M	
	expt	calcd	expt	calcd	expt	calcd
1.0		(1.8972)		(1.8782)		(2.0084)
1.4	0.960		1.062		0.395	
1.5	0.896	(1.2675)	0.890	(1.2255)	0.403	(1.3420)
2.0	0.712	(0.95269)	0.790	(0.94350)	0.4045	(1.0089)
4.0	0.403	(0.48045)	0.451	(0.47616)	0.3205	(0.50914)
6.0	0.283	(0.32303)	0.305	(0.32039)	0.262	(0.34256)
8.0	0.216	(0.24433)	0.265	(0.24250)	0.215	(0.25927)
10.0	0.170	(0.19710)	0.197	(0.19576)	0.181	(0.20929)
12.0	0.144	(0.16562)	0.1685	(0.16461)	0.156	(0.17598)
14.0	0.136	(0.14313)	0.146	(0.14235)	0.136	(0.15218)
16.0	0.110	(0.12626)	0.1252	(0.12566)	0.115	(0.13433)
18.0	0.0988	(0.11315)	0.112	(0.11268)	0.103	(0.12045)
20.0	0.090	(0.10205)	0.1036	(0.10230)	0.0948	(0.10935)
40.0	0.052	(0.055427)	0.0591	(0.055561)	0.0593	(0.059371)
60.0	0.037	(0.039674)	0.0421	(0.039951)	0.0443	(0.042681)
80.0	0.034	(0.031743)	0.0330	(0.032036)	0.0347	(0.034222)
100.0	0.0292	(0.026879)	0.02768	(0.027119)	0.0283	(0.028971)
140.0	0.0225	(0.020962)	0.02102	(0.021051)	0.02124	(0.022493)
180.0	0.0186	(0.017257)	0.01728	(0.017253)	0.01700	(0.018440)
220.0	0.0152	(0.014607)	0.01275	(0.014580)	0.01382	(0.015587)
260.0	0.0126	(0.012592)	0.01120	(0.012582)	0.01180	(0.013448)
290.0	0.0112	(0.011371)	0.01110	(0.011384)	0.01140	(0.012163)

The experimental χ_M values are corrected only for the diamagnetic susceptibility.

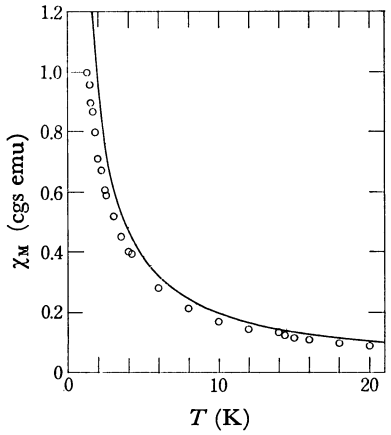

Fig. 4a. The molar magentic susceptibilities of $[(H_2O)_2Co\{(OH)_2Coen_2\}_2](SO_4)_2\cdot 5H_2O$ (cgs emu) *versus* temperatures lower than 20 K. ○: Experimental values which were corrected for the diamagnetic susceptibility. —: Calculated values with parameters, $g_{//}=5.915$, $g_{\perp}=3.566$, $\alpha=1.450$ and $\alpha'=1.950$.

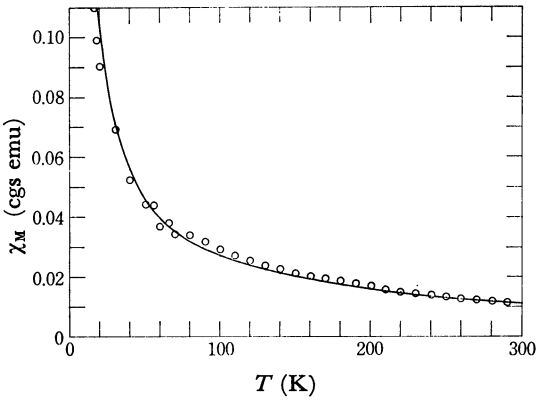

Fig. 4b. The molar magnetic susceptibilities of $[(H_2O)_2Co\{(OH)_2Coen_2\}_2](SO_4)_2\cdot 5H_2O$ (cgs emu) *versus* temperatures between 20 K and room temperature. ○: Experimental values which were corrected for the diamagnetic susceptibility. —: Calculated values with the same parameters as those in Fig. 4a.

Weiss law. In the case of a Co^{2+} ion co-ordinated by oxygen atoms in the form of an octahedron, it is known that the Co^{2+} ion has an effective spin of 1/2 at very low temperatures, where the spins are populated only in the lowest energy level. The Weiss constant of from −0.4 to −0.6 K, which was determined at liquid helium temperatures, was considered to be mainly due to the magnetic interaction. The high-frequency term was graphically obtained from data between 150 K and room temperature, that is, the extrapolation of the molar magnetic susceptibility as a function of the reciprocal temperature for $1/T\rightarrow 0$ was about 0.0007 cgs emu per mole. A similar extrapolation of the molar magnetic susceptibilities for $1/T\rightarrow 0$ from data between 14 and 20 K did not result in the same value, but it appears that the high-frequency term is not temperature independent suggesting that there are some excited levels of low excitation energy. The high-frequency term cannot be uniquely determined in these cases. On the other hand, the effective Bohr magneton number was also temperature dependent as

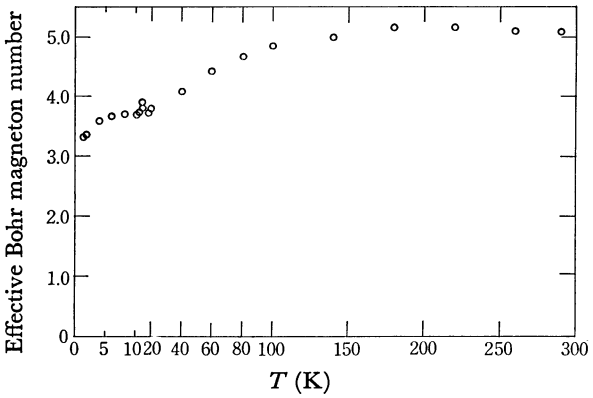

Fig. 5. The effective Bohr magneton numbers of $[(H_2O)_2Co\{(OH)_2Coen_2\}_2](SO_4)_2\cdot 5H_2O$ *versus* temperatures.

shown in Fig. 5. The value was about 5.1 at room temperature and gradually decreased to about 3.3 at 1.4 K. This decrease is more than that due to the antiferromagnetic interactions, indicating that the ground orbital level splits due to the ligand field of low symmetry.

The ESR derivative curve of this sample in powder form at 4.2 K is shown in Fig. 6. The signal intensity was weaker than that for $Co(NH_4)_2(SO_4)_2\cdot 6H_2O$ powder at 4.2 K, as shown in Fig. 7, but shapes of these two signals are quite similar. In $Co(NH_4)_2(SO_4)_2\cdot 6H_2O$, each Co^{2+} ion is surrounded by six oxygen atoms of coordinated water molecules with tetragonal symmetry and its g-values have been measured for single crystals by Bleaney and Ingram[10] to be $g_{\perp}=3.06\pm 0.06$ and $g_{//}=6.45\pm 0.13$. Simulations of the

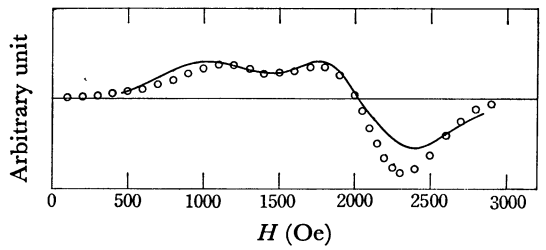

Fig. 6. ESR derivative curve of $[(H_2O)_2Co\{(OH)_2Coen_2\}_2](SO_4)_2\cdot 5H_2O$ on powder at 4.2 K. —: Experimental curve. ○: Simulation with parameters of $g_1=2.900$, $g_2=2.901$, $g_3=5.80$, $I=7/2$, $A_1=21.0$ Oe, $A_2=22.0$ Oe, $A_3=260.0$ Oe and line width=350 Oe.

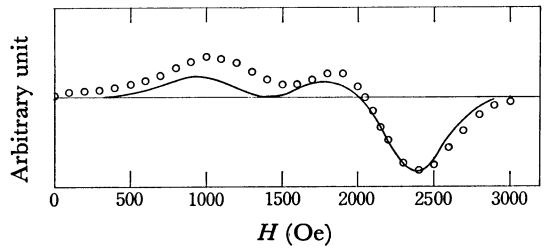

Fig. 7. ESR derivative curve of $Co(NH_4)_2(SO_4)_2\cdot 6H_2O$ on powder at 4.2 K. —: Experimental curve. ○: Simulation with parameters of $g_1=3.000$, $g_2=3.002$, $g_3=6.60$, $I=7/2$, $A_1=21.0$ Oe, $A_2=22.0$ Oe, $A_3=260.0$ Oe and line width=350 Oe.

ESR spectrum of $Co(NH_4)_2(SO_4)_2 \cdot 6H_2O$ powder with g-value, hyperfine constant and line width parameters according to the Kneübuhl method[11] were attempted to see if simulation is applicable to this sort of compound. Computations were performed with a FACOM 230—75 computer at Kyoto University using a program of Kuwada.[12] The best fit simulation for $Co(NH_4)_2(SO_4)_2 \cdot 6H_2O$ was obtained with the parameters: g-values, $g_1=3.000$, $g_2=3.002$, and $g_3=6.60$, hyperfine constants, $A_1=21.0$, $A_2=22.0$, and $A_3=260.0$ Oe and a line width of 350 Oe. The results are plotted in Fig. 7. The fair agreement between these g-values and those for single-crystal ESR proves that simulation can be used to estimate g-values. The hyperfine constants used are equal to those determined by Bleaney and Ingram[10] in single-crystal experiments. These constants were also used in simulations of $[(H_2O)_2Co\{(OH)_2Coen_2\}_2](SO_4)_2 \cdot 5H_2O$, $[(H_2O)_2Co\{(OH)_2Coen_2\}_2](SO_4)_2 \cdot 7H_2O$ and $[(H_2O)_2Co\{(OH)_2Coen_2\}_2](S_2O_6)_2 \cdot 5H_2O$. The line shapes of cobalt ammonium Tutton salt and $[(H_2O)_2Co\{(OH)_2Coen_2\}_2](SO_4)_2 \cdot 5H_2O$ are quite similar, and the best fit for the latter was obtained with $g_1=2.900$, $g_2=2.901$ and $g_3=5.80$ and line width of 350 Oe, as is shown in Fig. 6. Thus, the symmetry of a Co^{2+} ion in $[(H_2O)_2Co\{(OH)_2Coen_2\}_2](SO_4)_2 \cdot 5H_2O$ was concluded to be tetragonal as for the cobalt ammonium Tutton salt, though a difference of 0.001 between the values of g_1 and g_2 was necessary for a satisfactory fit. In Fig. 8, an example of simulations of ESR derivative curves is shown. All the curves were calculated for the same g_1 and g_3 values, that is, $g_1=3.060000$ and $g_3=6.450000$, but with the g_2 value varying from 3.060000 to 5.060000. It is worthwhile to note that when the anisotropy of the g values are almost tetragonal, the shapes of the ESR derivative curves are very sensitive to the anisotropy between the g_1 and g_2 values.

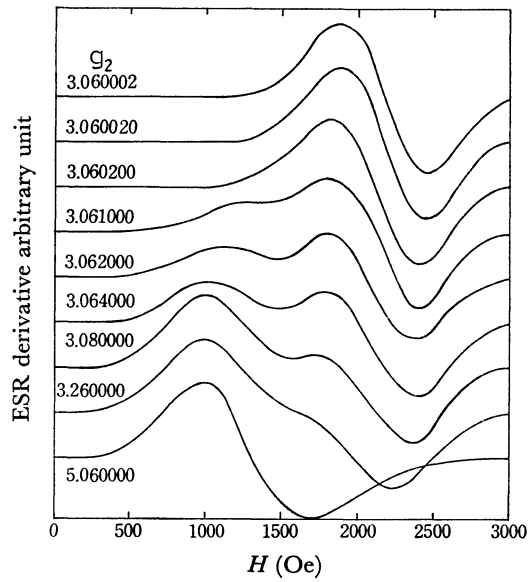

Fig. 8. Simulations of ESR derivative curves, where $g_1=3.060000$ and $g_3=6.450000$ are kept through all the cruves, but g_2 is varied from 3.060000 to 5.060000, which are written in the graph. The hyper-fine interaction is not considered.

The magnetic susceptibilities of Co^{2+} ions in the Tutton salts have been calculated by several authors[13] on the basis of the theory of Abragam and Pryce.[14] Calculations of the magnetic susceptibilities of $[(H_2O)_2Co\{(OH)_2Coen_2\}_2](SO_4)_2 \cdot 5H_2O$ were attempted assuming tetragonal symmetry and considering spin-orbit interaction in order to obtain a fit with the experimental values. The calculation was performed using the equations proposed by Bose *et al.*,[13] but with orbital levels up to the third level taken into consideration. Some good fits were obtained though the g-values were not completely equal to those from the ESR simulation. The best fit to the results are given in Table 3 in parentheses and are shown in Figs. 4a and 4b. The parameters of the best fit are $g_{//}=5.915$ and $g_{\perp}=3.566$ and $\alpha=1.450$ and $\alpha'=1.950$, where $-\alpha$ and $-\alpha'$ are the effective axial and perpendicular Landé factors,[14] respectively, in the spin-orbit coupling terms expressed by the fictitious orbital angular momentum. The energy

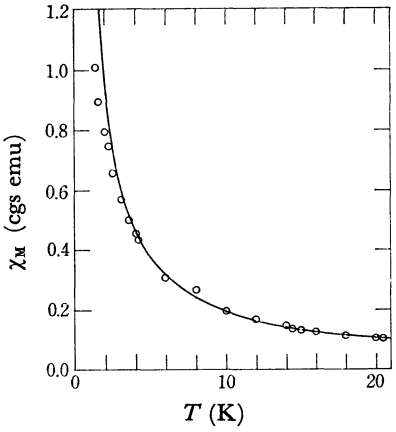

Fig. 9a. The molar magnetic susceptibilities of $[(H_2O)_2Co\{(OH)_2Coen_2\}_2](SO_4)_2 \cdot 7H_2O$ (cgs emu) as a function of temperatures (K) lower than 20 K. ○: Experimental values which were corrected for the diamagnetic susceptibility. —: Calculated values with parameters, $B_4^0=-2.00\ cm^{-1}$, $B_2^2=75.0\ cm^{-1}$, $B_2^0=40.0\ cm^{-1}$, $\alpha_x=1.62$, $\alpha_y=1.52$, $\alpha_z=1.35$, $g_x=4.126$, $g_y=5.961$ and $g_z=2.690$.

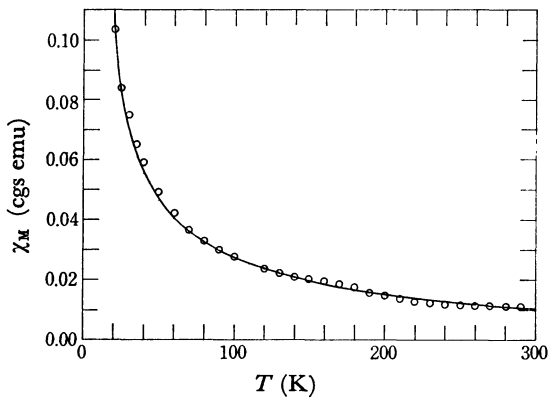

Fig. 9b. The molar magnetic susceptibilities of $[(H_2O)_2Co\{(OH)_2Coen_2\}_2](SO_4)_2 \cdot 7H_2O$ (cgs emu) as a function of temperatures between 20 K and room temperature. ○: Experimental values which were corrected for the diamagnetic susceptibility. —: Calculated values with the same parameters as those in Fig. 9a.

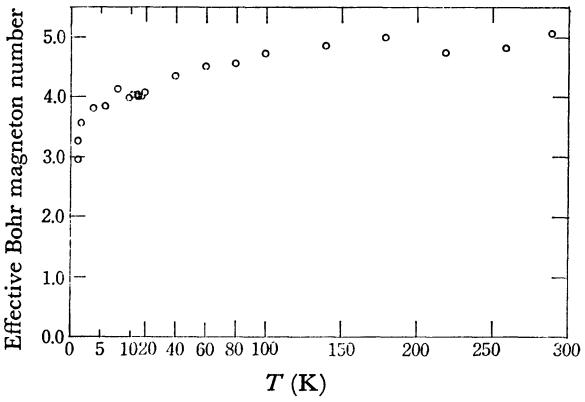

Fig. 10. The effective Bohr magneton numbers of $[(H_2O)_2Co\{(OH)_2Coen_2\}_2](SO_4)_2 \cdot 7H_2O$ *versus* temperatures.

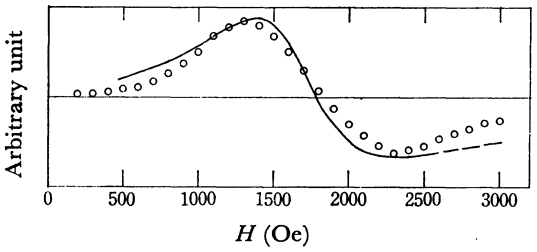

Fig. 11. ESR derivative curve of $[(H_2O)_2Co\{(OH)_2Coen_2\}_2](SO_4)_2 \cdot 7H_2O$ on powder at 1.3 K. —: Experimental curve. ○: Simulation with parameters of $g_1=2.00$, $g_2=3.00$, $g_3=4.50$, $I=7/2$, $A_1=21.0$ Oe, $A_2=22.0$ Oe, $A_3=260.0$ Oe, and line width=400 Oe.

difference between the ground level and the first-excited level is about 280 k, which is comparable to that of the Tutton salt.[13] If we follow the idea of the hexa coordination proposed by Werner,[1] it is reasonable to assume tetragonal symmetry.

The molar magnetic susceptibility of $[(H_2O)_2Co\{(OH)_2Coen_2\}_2](SO_4)_2 \cdot 7H_2O$ was close to that of $[(H_2O)_2Co\{(OH)_2Coen_2\}_2](SO_4)_2 \cdot 5H_2O$, as is seen in Figs. 9a and 9b and 10, and Table 3, but the ESR of the former is much more difficult to observe than that of the latter. The derivative curves of ESR were quite different, as is shown in Figs. 6 and 11. Because of the very broad line width, which seems to be more than 400 Oe, simulations would include numerous ambiguities. A calculated ESR derivative curve with g-values of 2.00, 3.00, and 4.50 and a line width of 400 Oe is shown in Fig. 11, this curve being one of the best fits though the g-values are unexpectedly small. This anisotropy of the g-values of a Co^{2+} ion in $[(H_2O)_2Co\{(OH)_2Coen_2\}_2](SO_4)_2 \cdot 7H_2O$ suggests that the ligandation of water molecules is different from that of penta hydrate. The Weiss constant of −0.6 to −0.7 K, which was obtained in the lowest temperature region, of the hepta hydrate is a little larger in absolute value than that of the penta hydrate. However, the hepta hydrate is, on the whole, considered to be more dilute for magnetic ions than the penta hydrate, suggesting some changes of the superexchange interaction paths. It was thought that the symmetry of the ligand field in the hepta hydrate is lower than that of the

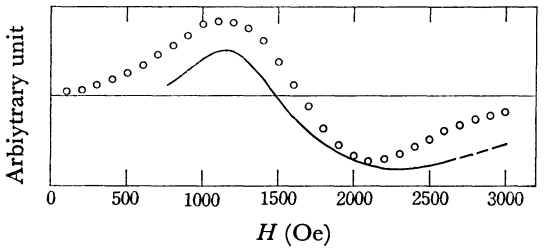

Fig. 12. ESR derivative curve of $[(H_2O)_2Co\{(OH)_2Coen_2\}_2](S_2O_6)_2 \cdot 5H_2O$ on powder at 4.2 K. —: Experimental curve. ○: Simulation with parameters of $g_1=2.30$, $g_2=5.20$, $g_3=5.80$, $I=7/2$, $A_1=21.0$ Oe, $A_2=22.0$ Oe $A_3=260.0$ Oe, and line width=600 Oe.

tetragonal from the symmetry of the g-values. On the other hand, the ESR derivative curve of $[(H_2O)_2Co\{(OH)_2Coen_2\}_2](S_2O_6)_2 \cdot 5H_2O$ was different from both the sulfate penta hydrate and the sulfate hepta hydrate, as is shown in Fig. 12. The simulation of this dithionate penta hydrate gave g-values of $g_1=2.30$, $g_2=5.20$, and $g_3=5.80$ with a width of 600 Oe. This anisotropy of the g-values is of the type $g_1<g_2\approx g_3$. A dithionate ion is larger in size than a sulfate ion, so it was supposed that $[(H_2O)_2Co\{(OH)_2Coen_2\}_2](S_2O_6)_2 \cdot 5H_2O$ would be magnetically more dilute than $[(H_2O)_2Co\{(OH)_2Coen_2\}_2](SO_4)_2 \cdot 5H_2O$. However, the observed magnetic susceptibility resulted in a negative Weiss constant having an absolute value larger than that of the penta hydrate and with a maximum near 2 K. The magnetic interactions may be operating *via* anions and some water molecules, and the dithionate ion does not result in a weaker linkage among the complex ions than does the sulfate ion in this case.

An attempt was made to calculate the magnetic susceptibilities of the dithionate penta hydrate and the sulfate hepta hydrate under the assumption of a rhombic ligand field symmetry. The method of calculation using the operator equivalents,[15] for which octahedral ligandation of oxygen atoms was assumed, is described in the appendix. The parameters for the best fit were as follows: for the dithionate penta hydrate, $\Delta r=8800$ cm^{-1}, $B_4^0=2.00$ cm^{-1}, $B_2^2=30.00$ cm^{-1}, $B_2^0=100.0$ cm^{-1}, $\alpha_x=1.81$, $\alpha_y=1.74$, $\alpha_z=0.90$, $g_x=5.044$, $g_y=5.768$ and $g_z=2.286$ and for the sulfate hepta hydrate, $\Delta r=8800$ cm^{-1}, $B_4^0=-2.00$ cm^{-1}, $B_2^2=75.00$ cm^{-1}, $B_2^0=40.0$ cm^{-1}, $\alpha_x=1.62$, $\alpha_y=1.52$, $\alpha_z=1.35$, $g_x=4.126$, $g_y=5.961$, and $g_z=2.690$. The calculated magnetic susceptibilities of the best fits are shown in Table 3 in parentheses and Figs. 9a and 9b, and 13a and 13b. As mentioned above, the dithionate penta hydrate showed that it has antiferromagnetic interactions, and therefore, in the lowest temperature region, the observed susceptibilities deviate from the calculated susceptibilities, for which magnetic interactions between magnetic ions are not taken into consideration. The discrepancy between the g-values from the ESR simulation and those from the magnetic susceptibility calculation is small in the case of $[(H_2O)_2Co\{(OH)_2Coen_2\}_2](S_2O_6)_2 \cdot 5H_2O$, however, the case of the sulfate hepta hydrate cannot be explained. If it is recalled that $[(H_2O)_2Ni\{(OH)_2Coen_2\}_2](SO_4)_2 \cdot 7H_2O$ has a rhombic ligand field for Ni^{2+} ion, a fairly good fit of the calculated magnetic

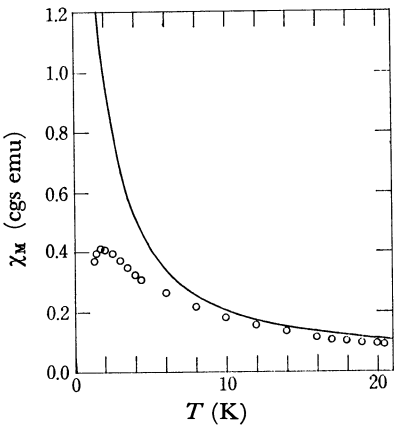

Fig. 13a. The molar magnetic susceptibilities of $[(H_2O)_2Co\{(OH)_2Coen_2\}_2](S_2O_6)_2 \cdot 5H_2O$ (cgs emu) as a function of temperatures (K) lower than 20 K. ○: Experimental values which were corrected for the diamagnetic susceptibility. —: Calculated values with parameters of $B_4^0=2.00\ cm^{-1}$, $B_2^2=30.00\ cm^{-1}$, $B_2^0=100.0\ cm^{-1}$, $\alpha_x=1.81$, $\alpha_y=1.74$, $\alpha_z=0.90$, $g_x=5.044$, $g_y=5.768$, and $g_z=2.286$.

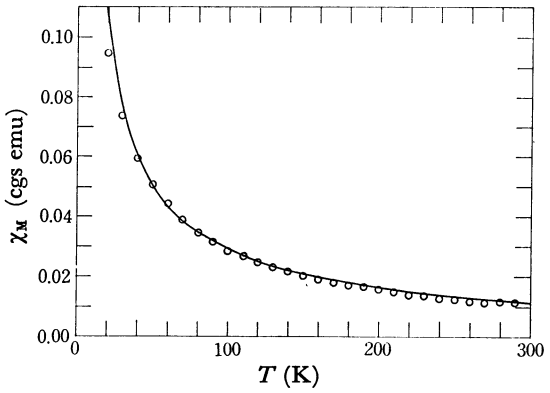

Fig. 13b. The molar magnetic susceptibilities of $[(H_2O)_2Co\{(OH)_2Coen_2\}_2](S_2O_6)_2 \cdot 5H_2O$ (cgs emu) as a function of temperatures (K) between 20 K and room temperature. ○: Experimental values which were corrected for the diamagnetic susceptibility. —: Calculated values with the same parameters to those in Fig. 13a.

susceptibility for $[(H_2O)_2Co\{(OH)_2Coen_2\}_2](SO_4)_2 \cdot 7H_2O$ under the assumption of rhombic anisotropy appears reasonable.

In conclusion, the magnetic properties of the $[(H_2O)_2M\{(OH)_2Coen_2\}_2]^{4+}$ ion, where M=Ni^{2+} or Co^{2+}, can be explained by those of the central divalent ion, that is, roughly speaking, the Co^{3+} ions in the wings are diamagnetic. In the solid state, the magnetic properties of the $[(H_2O)_2M\{(OH)_2Coen_2\}_2]^{4+}$ ion are not independent of the anion and crystalline water molecules, that is, the ligand field of sulfate penta hydrate was concluded to be tetragonal while those of sulfate hepta hydrate and dithionate penta hydrate were found to be rhombic, and the superexchange interactions were also to some extent dependent on the anions and crystalline water molecules.

This work was completed with the cooperation of Professor Masayasu Mori, Dr. Takashi Shibahara and Mr. Moriyoshi Hatta of Osaka City University, to whom the authors wish to express their deep gratitude for having provided the new compounds used in these experiments.

The authors wish to thank Professor Keiji Kuwada of Osaka University and Professor Shunichi Ohnishi of Kyoto University for valuable discussions on ESR simulation.

Appendix

Orbital energy levels, g-values of the lowest orbital level and molar magnetic susceptibilities for a ^4F state ion with a rhombic ligand field were calculated using the method of operator equivalents.[15] The operator equivalent method is based on the fact that, within a multiplet, the matrix elements of the potential function of the ion are proportional to the matrix elements of the appropriate polynomials of the orbital angular momentum operator.

The ligand field potential V that has been considered is

$$\begin{aligned} V &= V_K + V_{T2} + V_{T4} + V_{R2} \\ &= 20A_4(x^4+y^4+z^4-\frac{3}{5}r^4) + A_2^0(3z^2-r^2) \\ &\quad + A_4^0(35z^4-30z^2r^2+3r^4) + A_2^2(x^2-y^2), \end{aligned} \tag{3}$$

where V_K is the cubic potential function, V_{T2} and V_{T4} are the second- and fourth-order tetragonal potential functions, respectively, and V_{R2} is the second-order rhombic potential function. A_4, A_2^0, A_4^0, and A_2^2 are the coefficients of these potential functions, V_K, V_{T2}, V_{T4}, and V_{R2}, respectively. V_K is assumed to be much larger than V_{T2}, V_{T4}, and V_{R2}, so that the contributions from the latter terms can be treated as a perturbation. The matrix[16] of the cubic potential V_K for the orbital states $|M_L\rangle$ ($M_L=\pm3, \pm2, \pm1, 0$) is

$$60B_4 \times \begin{pmatrix} 3 & 0 & 0 & 0 & \sqrt{15} & 0 & 0 \\ 0 & -7 & 0 & 0 & 0 & 5 & 0 \\ 0 & 0 & 1 & 0 & 0 & 0 & \sqrt{15} \\ 0 & 0 & 0 & 6 & 0 & 0 & 0 \\ \sqrt{15} & 0 & 0 & 0 & 1 & 0 & 0 \\ 0 & 5 & 0 & 0 & 0 & -7 & 0 \\ 0 & 0 & \sqrt{15} & 0 & 0 & 0 & 3 \end{pmatrix}, \tag{4}$$

where $B_4=-2A_4\langle r^4\rangle/315$. The eigenstates of this secular matrix are the singlet Γ_2 and the triplets Γ_5 and Γ_4, for which the wave functions are

$$\varphi_1 = \sqrt{\frac{3}{8}}|-1\rangle+\sqrt{\frac{5}{8}}|+3\rangle = |\Gamma_4, 1\rangle,$$

$$\varphi_2 = -|0\rangle = |\Gamma_4, 0\rangle,$$

$$\varphi_3 = \sqrt{\frac{5}{8}}|-3\rangle+\sqrt{\frac{3}{8}}|+1\rangle = |\Gamma_4, -1\rangle,$$

$$\psi_1 = \sqrt{\frac{5}{8}}|-1\rangle-\sqrt{\frac{3}{8}}|3\rangle = |\Gamma_5, 1\rangle,$$

$$\psi_2 = \frac{1}{\sqrt{2}}(|2\rangle+|-2\rangle) = |\Gamma_5, 0\rangle,$$

$$\psi_3 = \sqrt{\frac{5}{8}}|1\rangle-\sqrt{\frac{3}{8}}|-3\rangle = |\Gamma_5, -1\rangle,$$

and

$$\chi = \frac{1}{\sqrt{2}}(|2\rangle-|-2\rangle) = |\Gamma_2, 0\rangle.$$

$$\begin{pmatrix} 6B_2^0+135B_4^0 & 0 & 6B_2^2 & -3\sqrt{15}(B_2^0+5B_4^0) & 0 & \sqrt{15}B_2^2 \\ 0 & -12B_2^0+360B_4^0 & 0 & 0 & 2\sqrt{15}B_2^2 & 0 \\ 6B_2^2 & 0 & 6B_2^0+135B_4^0 & \sqrt{15}B_2^2 & 0 & -3\sqrt{15}(B_2^0+5B_4^0) \\ -3\sqrt{15}(B_2^0+5B_4^0) & 0 & \sqrt{15}B_2^2 & 105B_4^0+\Delta_\Gamma & 0 & 0 \\ 0 & 2\sqrt{15}B_2^2 & 0 & 0 & -420B_4^0+\Delta_\Gamma & 0 \\ \sqrt{15}B_2^2 & 0 & -3\sqrt{15}(B_2^0+5B_4^0) & 0 & 0 & 105B_4^0+\Delta_\Gamma \end{pmatrix}, \quad (5)$$

Following the process introduced by Abragam and Pryce[14] for the case of ligand fields of low symmetry, we take into account the orbitals Γ_4 and Γ_5, but neglect the contribution from the Γ_2 orbital.

The matrix elements of V_{T2}, V_{T4}, and V_{R2} based on $\{\varphi_i\}$ and $\{\varphi_i\}$ $(i=1, 2, 3)$ are, if we set $B_2^0=-2A_2^0\langle r^2\rangle/105$, $B_2^2=-2A_2^2\langle r^2\rangle/105$, and $B_4^0=-2A_4^0\langle r^4\rangle/315$, where Δ_Γ is the separation between the Γ_4 and Γ_5 levels and is equal to $480|B_4|$. The orbital levels obtained by the diagonalization of (5) are shown in Fig. 14.

The components of the orbital angular momentum L based on $\{\varphi_i\}$ and $\{\varphi_i\}$ $(i=1, 2, 3)$ are represented as follows,

$$L_x=\frac{1}{2}\begin{pmatrix} 0 & \frac{-3}{2}\sqrt{2} & 0 & 0 & \sqrt{\frac{15}{2}} & 0 \\ \frac{-3}{2}\sqrt{2} & 0 & \frac{-3}{2}\sqrt{2} & -\sqrt{\frac{15}{2}} & 0 & -\sqrt{\frac{15}{2}} \\ 0 & \frac{-3}{2}\sqrt{2} & 0 & 0 & \sqrt{\frac{15}{2}} & 0 \\ 0 & -\sqrt{\frac{15}{2}} & 0 & 0 & \frac{\sqrt{2}}{2} & 0 \\ \sqrt{\frac{15}{2}} & 0 & \sqrt{\frac{15}{2}} & \frac{\sqrt{2}}{2} & 0 & \frac{\sqrt{2}}{2} \\ 0 & -\sqrt{\frac{15}{2}} & 0 & 0 & \frac{\sqrt{2}}{2} & 0 \end{pmatrix},$$

$$L_y=\frac{-i}{2}\begin{pmatrix} 0 & \frac{-3}{2}\sqrt{2} & 0 & 0 & -\sqrt{\frac{15}{2}} & 0 \\ \frac{3}{2}\sqrt{2} & 0 & \frac{-3}{2}\sqrt{2} & \sqrt{\frac{15}{2}} & 0 & -\sqrt{\frac{15}{2}} \\ 0 & \frac{3}{2}\sqrt{2} & 0 & 0 & \sqrt{\frac{15}{2}} & 0 \\ 0 & -\sqrt{\frac{15}{2}} & 0 & 0 & \frac{-\sqrt{2}}{2} & 0 \\ \sqrt{\frac{15}{2}} & 0 & -\sqrt{\frac{15}{2}} & \frac{\sqrt{2}}{2} & 0 & \frac{-\sqrt{2}}{2} \\ 0 & \sqrt{\frac{15}{2}} & 0 & 0 & \frac{\sqrt{2}}{2} & 0 \end{pmatrix},$$

and

$$L_z=\begin{pmatrix} \frac{-3}{2} & 0 & 0 & \frac{\sqrt{15}}{2} & 0 & 0 \\ 0 & 0 & 0 & 0 & 0 & 0 \\ 0 & 0 & \frac{3}{2} & 0 & 0 & \frac{-\sqrt{15}}{2} \\ \frac{\sqrt{15}}{2} & 0 & 0 & \frac{-1}{2} & 0 & 0 \\ 0 & 0 & 0 & 0 & 0 & 0 \\ 0 & 0 & \frac{-\sqrt{15}}{2} & 0 & 0 & \frac{1}{2} \end{pmatrix}. \quad (6)$$

The lowest three orbital states ξ_1, ξ_2, and ξ_3 in matrix (5) are given by

$$\xi_1=\mu_1\varphi_1+\mu_1'\varphi_3+\nu_1\phi_1+\nu_1'\phi_3,\ \xi_2=\mu_2\varphi_2+\nu_2\phi_2,$$
$$\text{and } \xi_3=\mu_3\varphi_1+\mu_3'\varphi_3+\nu_3\phi_1+\nu_3'\phi_3. \quad (7)$$

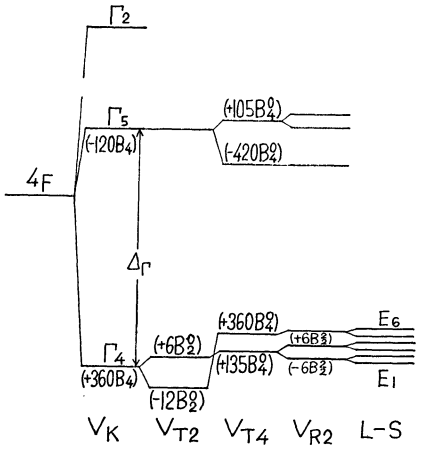

Fig. 14. Orbital energy level splittings of a ^4F state in a field of rhombic symmetry.

The components of the angular momentum based on $\{\xi_i\}$ $(i=1, 2, 3)$ are

$$L_x=\frac{1}{2}\begin{pmatrix} 0 & \rho_x & 0 \\ \rho_x & 0 & \rho_x' \\ 0 & \rho_x' & 0 \end{pmatrix},$$

$$L_y=\frac{-i}{2}\begin{pmatrix} 0 & \rho_y' & 0 \\ -\rho_y' & 0 & \rho_y \\ 0 & -\rho_y & 0 \end{pmatrix},$$

and

$$L_z=\begin{pmatrix} \rho_z' & 0 & \rho_z \\ 0 & 0 & 0 \\ \rho_z & 0 & \rho_z'' \end{pmatrix}, \quad (8)$$

where ρ_v, ρ_v', and ρ_v'' $(v=x, y, z)$ are, using (7),

$$\rho_x=\frac{-3\sqrt{2}}{2}\mu_2(\mu_1+\mu_1')+\sqrt{\frac{15}{2}}\{\nu_2(\mu_1+\mu_1')-\mu_2(\nu_1+\nu_1')\}+\frac{\sqrt{2}}{2}\nu_2(\nu_1+\nu_1'),$$

$$\rho_x'=\frac{-3\sqrt{2}}{2}\mu_2(\mu_3+\mu_3')+\sqrt{\frac{15}{2}}\{\nu_2(\mu_3+\mu_3')-\mu_2(\nu_3+\nu_3')\}+\frac{\sqrt{2}}{2}\nu_2(\nu_3+\nu_3'),$$

$$\rho_y=\frac{3\sqrt{2}}{2}\mu_2(\mu_3-\mu_3')+\sqrt{\frac{15}{2}}\{\nu_2(\mu_3-\mu_3')+\mu_2(\nu_3-\nu_3')\}+\frac{\sqrt{2}}{2}\nu_2(\nu_3-\nu_3'),$$

$$\rho_y'=\frac{3\sqrt{2}}{2}\mu_2(-\mu_1+\mu_1')+\sqrt{\frac{15}{2}}\{\nu_2(-\mu_1+\mu_1')+\mu_2(-\nu_1+\nu_1')\}+\frac{\sqrt{2}}{2}\nu_2(-\nu_1+\nu_1'),$$

$$\rho_z = \frac{-3}{2}(\mu_1\mu_3-\mu_1'\mu_3')+\sqrt{\frac{15}{2}}(\mu_1\nu_3+\nu_1\mu_3-\mu_1'\nu_3'-\nu_1'\mu_3') -\frac{1}{2}(\nu_1\nu_3-\nu_1'\nu_3'),$$

$$\rho_z' = \frac{-3}{2}(\mu_1^2-\mu_1'^2)+\sqrt{15}(\mu_1\nu_1-\mu_1'\nu_1')-\frac{1}{2}(\nu_1^2-\nu_1'^2),$$

and $$\rho_z'' = \frac{-3}{2}(\mu_3^2-\mu_3'^2)+\sqrt{15}(\mu_3\nu_3-\mu_3'\nu_3')-\frac{1}{2}(\nu_3^2-\nu_3'^2).$$

The solution of the secular equation shows that $\mu_1'=\mu_1, \nu_1'=\nu_1$, $\mu_3'=-\mu_3$, and $\nu_3'=-\nu_3$ in the case of orthorhombic ligand fields, and therefore,

$$\begin{aligned}\xi_1 &= \mu_1(\varphi_1+\varphi_3)+\nu_1(\psi_1+\psi_3),\\ \xi_2 &= \mu_2\varphi_2+\nu_2\psi_2,\\ \text{and}\quad \xi_3 &= \mu_3(\varphi_1-\varphi_3)+\nu_3(\psi_1-\psi_3).\end{aligned} \tag{9}$$

If we define the α_v ($v=x, y, z$) as follows

$$\alpha_x = \frac{-\rho_x}{2} = \frac{3\sqrt{2}}{2}\mu_1\mu_2-\sqrt{\frac{15}{2}}\{\mu_1\nu_2-\mu_2\nu_1\}-\frac{\sqrt{2}}{2}\nu_1\nu_2,$$

$$\alpha_y = \frac{\rho_y}{2} = \frac{3\sqrt{2}}{2}\mu_2\mu_3+\sqrt{\frac{15}{2}}\{\nu_2\mu_3+\nu_3\mu_2\}+\frac{\sqrt{2}}{2}\nu_2\nu_3,$$

and $$\alpha_z = -\rho_z = 3\mu_1\mu_3-\sqrt{15}(\mu_1\nu_3+\nu_1\mu_3)+\nu_1\nu_3, \tag{10}$$

and it is known that

$$\rho_x' = \rho_y' = \rho_z' = \rho_z'' = 0,$$

then the components of the angular momentum can be written as follows,

$$L_x = -\alpha_x\begin{bmatrix}0&1&0\\1&0&0\\0&0&0\end{bmatrix} = -\alpha_x l_x',$$

$$L_y = -\alpha_y\begin{bmatrix}0&0&0\\0&0&i\\0&-i&0\end{bmatrix} = -\alpha_y l_y',$$

and $$L_z = -\alpha_z\begin{bmatrix}0&0&1\\0&0&0\\1&0&0\end{bmatrix} = -\alpha_z l_z', \tag{11}$$

where $l_x'^2+l_y'^2+l_z'^2 = l(l+1) = 2,\ (l=1)$.

The α_x, α_y, and α_z indicate the contributions from the Γ_5 orbital level. When there is no contribution from the Γ_5 level, that is, when the lowest triplet Γ_4 state consists of only the wave functions $\{\varphi_1\}$, α_x, α_y, and α_z are

$$\alpha_x = \alpha_y = \alpha_z = 1.5.$$

The potential function (3) is replaced by the equivalent angular momentum operators[15] as follows,

$$\begin{aligned}\hat{V} &= \hat{V}_K+\hat{V}_{T2}+\hat{V}_{T4}+\hat{V}_{R2}\\ &= B_4(O_4^0+5O_4^4)+B_2^0O_2^0+B_4^0O_4^0+B_2^2O_2^2,\end{aligned} \tag{12}$$

where $B_4 = \langle L\|\beta\|L\rangle A_4\langle r^4\rangle$,
$B_2^0 = \langle L\|\alpha\|L\rangle A_2^0\langle r^2\rangle$,
$B_4^0 = \langle L\|\beta\|L\rangle A_4^0\langle r^4\rangle$,
and $B_2^2 = \langle L\|\alpha\|L\rangle A_2^2\langle r^2\rangle$.

$\langle L\|\alpha\|L\rangle$ and $\langle L\|\beta\|L\rangle$ are the proportional coefficients,[16] $-2/105$ and $-2/315$, respectively, and $\langle r_j\rangle$ is the average of r_j over the radial part of the wave function. O_3^0, O_2^2, O_4^0, and O_4^4 can be written using the orbital angular momentum operator L, thus

$$\begin{aligned}O_2^0 &= 3L_z^2-L(L+1),\\ O_2^2 &= \frac{1}{2}(L_+^2+L_-^2),\\ O_4^0 &= 35L_z^4-30L(L+1)L_z^2+25L_z^2\\ &\quad -6L(L+1)+3L^2(L+1)^2,\\ \text{and}\quad O_4^4 &= \frac{1}{2}(L_+^4+L_-^4).\end{aligned} \tag{13}$$

Using the α_x, α_y, and α_z mentioned above and $l=1$, the V_{T2}, V_{T4}, and V_{R2} (in Eq. 12) can be written as follows,

$$\begin{aligned}\hat{V}_{T2} &= \frac{1}{4}B_2^0Q_2^0,\\ \hat{V}_{T4} &= B_4^0Q_4^0,\\ \hat{V}_{R2} &= \frac{1}{4}B_2^2Q_2^2,\end{aligned} \tag{14}$$

where $Q_2^0 = (8\alpha_z^2+2p)l_z^2-4p-q(l_+^2+l_-^2)$,
$Q_4^0 = u_1l_z^2+u_2(l_+^2+l_-^2)+u_3$,
$Q_2^2 = p(l_+^2+l_-^2)-2ql_z^2+4q$,
$p = \alpha_x^2+\alpha_y^2$,
$q = \alpha_x^2-\alpha_y^2$,
$u_1 = 8\alpha_z^4-12p\alpha_z^2+19\alpha_z^2+3p-\frac{9}{4}p^2+\frac{3}{4}q^2$,
$u_2 = \frac{3}{2}q\left(\frac{p}{2}-4\alpha_z^2-1\right)$,
and $u_3 = 3p(p-2)$.

The first-order perturbation Hamiltonian containing the spin-orbit interaction is

$$\begin{aligned}\mathcal{H} &= \frac{1}{4}B_2^0Q_2^0+B_4^0Q_4^0+\frac{1}{4}B_2^2Q_2^2\\ &\quad -\lambda(\alpha_xl_xS_x+\alpha_yl_yS_y+\alpha_zl_zS_z).\end{aligned} \tag{15}$$

When the rhombic symmetry is taken into account, $m(=l_z+S_z)$ is not a good quantum number. The secular matrix of Eq. 15 represented in the basis set of $|l_z, S_z\rangle$ is

$$\begin{array}{cccccc}|-1,\frac{3}{2}\rangle & |-1,\frac{-1}{2}\rangle & |1,\frac{3}{2}\rangle & |1,\frac{-1}{2}\rangle & |0,\frac{1}{2}\rangle & |0,\frac{-3}{2}\rangle\\ |1,\frac{-3}{2}\rangle & |1,\frac{1}{2}\rangle & |-1,\frac{-3}{2}\rangle & |-1,\frac{1}{2}\rangle & |0,\frac{-1}{2}\rangle & |0,\frac{3}{2}\rangle\end{array}$$

$$\begin{pmatrix}
T_f+R_f+\frac{3}{2}\alpha_z\lambda & 0 & \frac{1}{2}(pB_2^2-qB_2^0)+2u_2B_4^0 & 0 & \frac{-\sqrt{6}}{4}r\lambda & 0\\
0 & T_f+R_f-\frac{1}{2}\alpha_z\lambda & 0 & \frac{1}{2}(pB_2^2-qB_2^0)+2u_2B_4^0 & \frac{-\sqrt{2}}{2}s\lambda & \frac{-\sqrt{6}}{4}r\lambda\\
\frac{1}{2}(pB_2^2-qB_2^0)+2u_2B_4^0 & 0 & T_f+R_f-\frac{3}{2}\alpha_z\lambda & 0 & \frac{-\sqrt{6}}{4}s\lambda & 0\\
0 & \frac{1}{2}(pB_2^2-qB_2^0)+2u_2B_4^0 & 0 & T_f+R_f+\frac{1}{2}\alpha_z\lambda & \frac{-\sqrt{2}}{2}r\lambda & \frac{-\sqrt{6}}{4}s\lambda\\
\frac{-\sqrt{6}}{4}r\lambda & \frac{-\sqrt{2}}{2}s\lambda & \frac{-\sqrt{6}}{4}s\lambda & \frac{-\sqrt{2}}{2}r\lambda & 0 & 0\\
0 & \frac{-\sqrt{6}}{4}r\lambda & 0 & \frac{-\sqrt{6}}{4}s\lambda & 0 & 0
\end{pmatrix}, \tag{16}$$

where $$T_f = \left(2\alpha_z^2 + \frac{1}{2}p\right)B_2^0 + u_1 B_4^0,$$

$$R_f = -\frac{1}{2}qB_2^2,$$

$$r = \alpha_x + \alpha_y,$$

and $$s = \alpha_x - \alpha_y.$$

The six Kramers doublets, which are deduced from the lowest orbital triplet, are obtained through the diagonalization of (16). The energy levels of the six Kramers doublets are expressed as E_i ($i=1, 2, ..., 6$) and their wave functions as $\Phi_{\pm i}$ ($i=1, 2, ..., 6$). Then

$$\Phi_{+i} = \sum_{j=1}^{6} C_{ij}\zeta_j,$$

and $$\Phi_{-i} = \sum_{j=1}^{6} C_{ij}\zeta_j^*, \qquad (17)$$

where $\{\zeta_j\}$ is the base of the secular matrix (16) and its coefficient of linear combination, C_{ij}, can be determined from the solution of the secular equation. The g factors of the lowest Kramers doublet are given as follows:

$$\begin{aligned}
g_x &= 2\langle\Phi_{+1}|-\alpha_x l_x + 2S_x|\Phi_{-1}\rangle \\
&= -2\sqrt{2}\,\alpha_x(C_{11}C_{16}+C_{12}C_{15}+C_{13}C_{16}+C_{14}C_{15}) \\
&\quad +4\sqrt{3}\,(C_{11}C_{14}+C_{12}C_{13}+C_{15}C_{16})+8C_{12}C_{14}+4C_{15}^2, \\
g_y &= 2\langle\Phi_{+1}|-\alpha_y l_y + 2S_y|\Phi_{-1}\rangle \\
&= -2\sqrt{2}\,\alpha_y(-C_{11}C_{16}-C_{12}C_{15}+C_{13}C_{16}+C_{14}C_{15}) \\
&\quad +4\sqrt{3}\,(C_{11}C_{14}+C_{12}C_{13}-C_{15}C_{16})-8C_{12}C_{14}+4C_{15}^2, \\
g_z &= 2\langle\Phi_{+1}|-\alpha_z l_z + 2S_z|\Phi_{+1}\rangle \\
&= 2[(C_{11}^2+C_{12}^2-C_{13}^2-C_{14}^2)\alpha_z+3(C_{11}^2+C_{13}^2-C_{16}^2) \\
&\quad -C_{12}^2-C_{14}^2+C_{15}^2]. \qquad (18)
\end{aligned}$$

The magnetic susceptibility per mole is given by

$$\chi_v = \frac{N\beta^2}{Z}\left(\frac{G^v}{kT}+2G'^v\right), \quad (v=x, y, z)$$

where $$G^v = \sum_{i=1}^{6} G_i^v \exp\frac{-(E_i-E_1)}{kT},$$

$$G_i^v = \sum_{\pm}|\langle\Phi_{\pm i}|-\alpha_v l_v + 2S_v|\Phi_{\pm i}\rangle|^2,$$

$$G'^v = \sum_{i=1}^{6} G'^v_i \exp\frac{-(E_i-E_1)}{kT},$$

$$G'^v_i = \sum_{j(\neq i)}^{6} G'^v_{ij},$$

$$G'^v_{ij} = \sum_{\pm}\frac{|\langle\Phi_{\pm i}|-\alpha_v l_v + 2S_v|\Phi_{\pm j}\rangle|^2}{E_j-E_i},$$

and $$Z = 2\sum_{i=1}^{6}\exp\frac{-(E_i-E_1)}{kT}.$$

The G_i^v and G'^v_{ij} are

$$\begin{aligned}
G_i^x &= 2[-\sqrt{2}\,\alpha_x(C_{i1}C_{i6}+C_{i2}C_{i5}+C_{i3}C_{i6}+C_{i4}C_{i5}) \\
&\quad +2\sqrt{3}\,(C_{i1}C_{i4}+C_{i2}C_{i3}+C_{i5}C_{i6})+4C_{i2}C_{i4}+2C_{i5}^2]^2, \\
G_i^y &= 2[\sqrt{2}\,\alpha_y(C_{i1}C_{i6}+C_{i2}C_{i5}-C_{i3}C_{i6}-C_{i4}C_{i5}) \\
&\quad +2\sqrt{3}\,(C_{i1}C_{i4}+C_{i2}C_{i3}-C_{i5}C_{i6})-4C_{i2}C_{i4}+2C_{i5}^2]^2, \\
G_i^z &= 2[\alpha_z(C_{i1}^2+C_{i2}^2-C_{i3}^2-C_{i4}^2)+3(C_{i1}^2+C_{i3}^2-C_{i6}^2) \\
&\quad -C_{i1}^2-C_{i4}^2+C_{i5}^2]^2,
\end{aligned}$$

$$\begin{aligned}
G'^x_{ij} &= \frac{2}{E_j-E_i}[\sqrt{3}\,(C_{i1}C_{j4}+C_{i4}C_{j1}+C_{i2}C_{j3}+C_{i3}C_{j2} \\
&\quad +C_{i5}C_{j6}+C_{i6}C_{j5})-\frac{\sqrt{2}}{2}\alpha_x(C_{i1}C_{j6}+C_{i6}C_{j1}+C_{i2}C_{j5} \\
&\quad +C_{i5}C_{j2}+C_{i3}C_{j6}+C_{i6}C_{j3}+C_{i4}C_{j5}+C_{i5}C_{j4}) \\
&\quad +2(C_{i2}C_{j4}+C_{i4}C_{j2}+C_{i5}C_{j5})]^2,
\end{aligned}$$

$$\begin{aligned}
G'^y_{ij} &= \frac{2}{E_j-E_i}[\sqrt{3}\,(C_{i1}C_{j4}+C_{i4}C_{j1}+C_{i2}C_{j3}+C_{i3}C_{j2} \\
&\quad -C_{i5}C_{j6}-C_{i6}C_{j5})+\frac{\sqrt{2}}{2}\alpha_y(C_{i1}C_{j6}+C_{i6}C_{j1}+C_{i2}C_{j5} \\
&\quad +C_{i5}C_{j2}-C_{i3}C_{j6}-C_{i6}C_{j3}-C_{i4}C_{j5}-C_{i5}C_{j4}) \\
&\quad -2(C_{i2}C_{j4}+C_{i4}C_{j2}-C_{i5}C_{j5})]^2,
\end{aligned}$$

$$\begin{aligned}
G'^z_{ij} &= \frac{2}{E_j-E_i}[\alpha_z(C_{i1}C_{j1}+C_{i2}C_{j2}-C_{i3}C_{j3}-C_{i4}C_{j1}) \\
&\quad +3(C_{i1}C_{j1}+C_{i3}C_{j3}-C_{i6}C_{j6})-C_{i2}C_{j2}-C_{i4}C_{j4} \\
&\quad +C_{i5}C_{j5}]^2.
\end{aligned}$$

We must estimate the error in the operator equivalent method used in the above calculation. The method is valid for the lowest multiplet ^4F. The effect of mixing with the upper state of a different multiplet, *e.g.*, the Γ'_4 state arising from ^4P, can be estimated from the matrix element of $\hat{V}_{T2}+\hat{V}_{T4}+\hat{V}_{R2}$ between the lowest and the excited multiplets. Roughly, the contribution of the mixing with the upper mul-

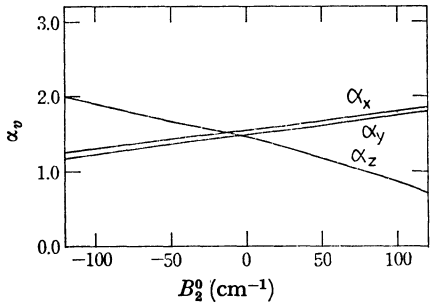

Fig. 15. α_v as a function of B_2^0. The graph is calculated for $\Delta\Gamma=8800$ cm^{-1}, $B_4^0=2.00$ cm^{-1}, and $B_2^2=30.0$ cm^{-1}.

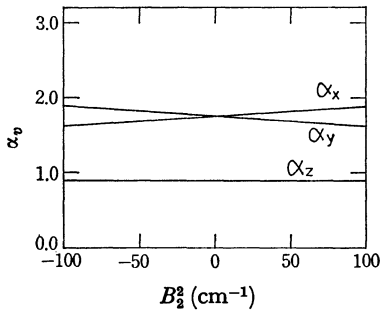

Fig. 16. α_v as a function of B_2^2, where $\Delta\Gamma=8800$ cm^{-1}, $B_2^0=100$ cm^{-1} and $B_4^0=2.00$ cm^{-1} were used.

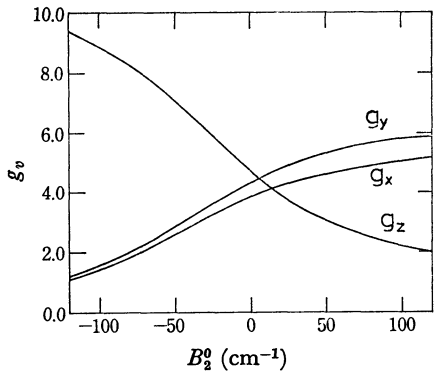

Fig. 17. g_v as a function of B_2^0 where $\Delta\Gamma=8800$ cm^{-1}, $B_4^0=2.00$ cm^{-1}, and $B_2^2=30.0$ cm^{-1} were used.

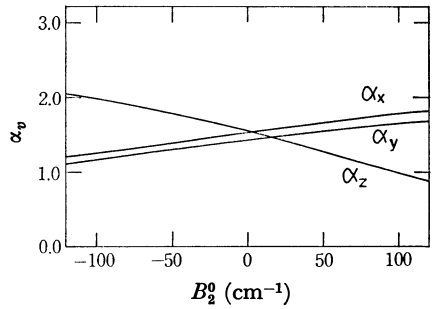

Fig. 18. α_v as a function of B_2^0, where $\Delta_\Gamma=8800$ cm^{-1}, $B_4^0=-2.00$ cm^{-1}, and $B_4^0=75.0$ cm^{-1} were used.

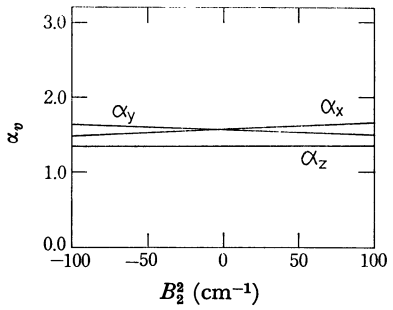

Fig. 19. α_v as a function of B_2^2, where $\Delta_\Gamma=8800$ cm^{-1}, $B_2^0=40.0$ cm^{-1}, and $B_4^0=-2.00$ cm^{-1} were used.

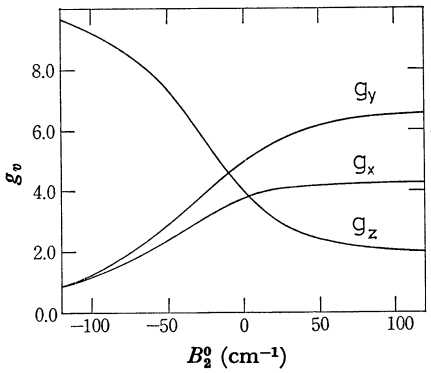

Fig. 20. g_v as a function of B_2^0, where $\Delta_\Gamma=8800$ cm^{-1}, $B_4^0=-2.00$ cm^{-1} and $B_2^2=75.0$ cm^{-1} were used.

tiplet to $\Delta\alpha$, the difference between α_v and 1.5, will be of the order of the ratio of the matrix element $\langle L=3|\hat{V}_{T2}+\hat{V}_{T4}+\hat{V}_{R2}|L\neq 3\rangle$ to the energy difference between the multiplets. Within the lowest multiplet, the more the Γ_5 level is separated from the Γ_4 level, the less the deviation of α_v from 1.5. The case of $\alpha_v=1.5$ has been analyzed by Uryû *et al.*[17] who dealt with $CoCl_2\cdot 6H_2O$. The same g-values as those of the Co Tutton salt[9] are found with the following parameters: $\alpha_x=\alpha_y=\alpha_v=1.5$, $B_4^0=2.00$ cm^{-1}, $B_2^0=-70.0$ cm^{-1}, and $B_2^2=0.00$ cm^{-1}.

In Figs. 15 and 16, α_v, $(v=x, y, z)$, is plotted as a function of B_2^0 and B_2^2, respectively. In Fig. 17, g_v, $(v=x, y, z)$, is shown as a function of B_2^0. In Figs. 15—17, the functions are calculated using the parameters, $\Delta_\Gamma=8800$ cm^{-1}, $B_4^0=2.00$ cm^{-1} and $B_2^0=100$ cm^{-1} or $B_2^2=30.0$ cm^{-1}, that is, those which showed the best fit for $[(H_2O)_2Co\{(OH)_2Coen_2\}_2](S_2O_6)_2\cdot 5H_2O$. In Figs. 18—20, similar calculations are shown using the parameters, $\Delta_\Gamma=8800$ cm^{-1}, $B_4^0=-2.00$ cm^{-1}, and $B_2^0=40.0$ cm^{-1} or $B_2^2=75.0$ cm^{-1}, that is, those which showed the best fit for $[(H_2O)_2Co\{(OH)_2Coen_2\}_2](SO_4)_2\cdot 7H_2O$.

Numerical computations in the appendix and those of the magnetic susceptibilities were performed with a FACOM 230—45 computer at the Computer Center of Kyushu University.

References

1) A. Werner, *Berichte*, **40**, 4426 (1907).
2) L. Cambi, *Atti. accad. nazl. Lincei, Rend., classe sci. fis., mat. e nat.*, **18**, 581 (1955) and C. A. **50**, 5347d (1956).
3) G. H. Jonker and J. H. Van Santen, *Physica*, **16**, 337, 599 (1950); J. B. Goodenough, *Phys. Rev.*, **100**, 564 (1955); P. W. Anderson and H. Hasegawa, *ibid.*, **100**, 675 (1955).
4) D. C. Jicha and D. H. Busch, *Inorg. Chem.*, **1**, 872, 878 (1962); D. H. Busch and D. C. Jicha, *ibid.*, **1**, 884 (1962); P. S. Poskozim, R. Shute, R. Taylor, and J. Wysocki, *J. Inorg. Nucl. Chem.*, **55**, 687 (1973).
5) M. Mori, M. Hatta, and T. Shibahara, *Proc. XV I. C. C. C.*, **I**, 272 (1973); M. Hatta, T. Shibahara, and M. Mori, to be published.
6) C. T. Linder, Research Report, R-94433-2-A (Westinghouse Research Laboratories).
7) A. V. Jagnnadham, *Proc. Rajasthan Acad. Sci.*, **1**, 6 (1950); C. A., **45**, 9948 (1951).
8) J. H. E. Griffiths and J. Owen, *Proc. R. Soc. London, Ser. A*, **213**, 459 (1952).
9) T. Haseda and M. Date, *J. Phys. Soc. Jpn.*, **13**, 175 (1958).
10) B. Bleaney and D. J. E. Ingram, *Proc. R. Soc. London, Ser. A*, **208**, 143 (1951).
11) F. K. Kneubühl, *J. Chem. Phys.*, **33**, 1074 (1960).
12) K. Kuwada, "Saikin no Bunsekikagaku," Vol. 20, Kagaku Dojin, Kyoto, p. 123.
13) K. Kambe, *Prog. Theor. Phys.*, **7**, 15 (1952); N. Uryû, *J. Phys. Soc. Jpn.*, **11**, 770 (1956); A. Bose, A. S. Chakravarty, and R. Chatterjee, *Proc. R. Soc. London, Ser. A*, **261**, 431 (1961),
14) A. Abragam and M. H. L. Pryce, *Proc. R. Soc. London, Ser. A*, **206**, 173 (1951).
15) K. W. H. Stevens, *Proc. Phys. Soc. London*, **A65**, 209 (1952).
16) H. Kamimura, S. Sugano, and Y. Tanabe, "Ligand Field Theory and Its Applications," 2nd ed., Syokabo, Tokyo (1970); A. Abragam and B. Bleaney, "Electron Paramagnetic Resonance of Transition Ions," Clarendon Press, Oxford (1970); K. Osaki and N. Uryû, *Technology Reports of the Kyushu Univ.*, **47**, 575 (1974).
17) N. Uryû, J. Skalyo, Jr., and S. A. Friedberg, *Phys. Rev.*, **144**, 689 (1966).